Supporting Information

Anti-cancers activities of the metal-based complexes by regulating VEGF/VEGFR2 signaling pathway and apoptosis related factors Bcl-2, Bax, and Caspase-9 to inhibit angiogenesis and induce apoptosis

Xiu-Ying Qin,*[a1,b] Ya-Nan Wang,[a1] Han-Fu Liu, [a1] Zhao-Hui Luo,[a1] Pei-Lu Zhang,[a1] Li-Fang Huang[a1]and Mei-Rong Liu*,[a2]

[a] *College of Pharmacy[1], Department of Foreign Languages Teaching [2], Guilin Medical University, Guangxi Guilin, 541004, China*

[b] *Guangxi Key Laboratory of Early Prevention and Treatment for Regional High Frequency Tumor, Guangxi Medical University, Nanning, 530021, China*

** Corresponding Author: xyqin6688@163.com*； 79521059@qq.com

Experimental Procedures

Instruments. IR spectrums were taken on an IRAffinity-1 FT-IR spectrometer with KBr pallets in the range of 4000～400 cm^{-1}. The elemental analyses for C, H and N were performed on a Perkin-Elmer 2400C elemental analyzer. The crystal structures were determined by a four-circle CCD diffractometer(SuperNova, Single source at offset, Eos). Apoptosis assay were determined by BD FACSAriaⅢ. Migration and tube formation assays of HUVECs were photographed with a bright field of inverted fluorescence phase contrast microscope(OLYMPUS IXTIFL, Japan). Cells were cultured in a CO_2 incubator(311, Thermo, USA). Cells were observed with a inverted microscope(OLYMPUS ckx31, Japan). Ultrasonic cell fragmentation apparatus (VCX-130, Sonics, USA), high-speed refrigeration centrifuge (LegendRT-Plus,Thermo, USA), pure water ultra-pure water system (Elix3+30L+3YNERGY, Millipore, USA), high-speed centrifuge(Mini Spin, Eppendorf, Germany), protein transfer membrane system(TE22, GE, USA), protein electrophoresis tank(DYCZ-24DN, Beijing LiuYi, China), rockers(TS-1000, Lin bell, jiangsu province, China), and gel imaging system UV projector(ZF-4, Shanhhai, China), were used in western blot assays.

Materials. Solvents and chemicals obtained from commercial sources were of reagent grade and were used without further purification unless specially noted. All the reagents used for syntheses of target complexes posses ≥97%purity. 5-Bromo-3-methoxy-salicylaldehyde reagent was purchased from Alfa Aesar. MTT, penicillin/streptomycin, and dimethylsulfoxide was purchased from Sigma-Aldrich, USA. Dulbecco's modified eagle medium (DMEM, Gibco), RPMI-1640 medium(Gibco), Fetal bovine serum (FBS, GEMINI), pancreatic enzyme(Gibco), cell culture plates (Corning), Anti-

VEGFR2, Anti-phospho-VEGFR2, Anti-FAK(D2R2E), Anti-phospho-FAK(Tyr397), Anti-Akt(pan), Anti-phospho-Akt(Thr308),Anti-Erk1/2(p42/44), and Anti-phospho-Erk1/2(Cell Signaling Technology) were used. GAPDH antibodies were procured from Thermo Scientific. The fertile chicken eggs were purchased from a Poultry Station, Guilin, China. Annexin V/PI apoptosis kit was purchased from BD Bioscience. HUVECs, HeLa, and C33A cell lines were purchased from Shanghai oulu biological technology co., ltd. Vascular endothelial growth factor(VEGF) was purchased from Sangon Biotech (Shanghai) Co., Ltd. Cell culture: HUVECs were cultured in DMEM medium supplemented with FBS(10%), penicillin(100 μg/mL), and streptomycin (100 μg/mL); C33A cells were cultured in DMEM medium supplemented with FBS(15%), penicillin (100 μg/mL), and streptomycin (100 μg/mL); HeLa cells were cultured in RPMI-1640 medium supplemented with FBS(10%), penicillin (100 μg/mL), and streptomycin (100 μg/mL). They were incubated at 37℃ in a humidified incubator with 5 % CO_2 and 95 % air, and the medium was changed thrice weekly. The animal experiments were carried out in experiment animal center, SPF experimental animal lab, Guilin Medical University. None of the three metal-based complexes dissolve easily in water. They were dissolved by dimethylsulfoxide and diluted them with ultra-pure water. The DMSO volume was limited by less than 0.5% in cell experiments. The three metal-based complexes in the mixture of dimethylsulfoxide and ultra-pure water showed no change in color and no precipitation within 10 days, indicating that they were very stable.

Supporting Tables

Table S1. Crystal data and structure refinement parameters for Cu-1 and Co-1.

Parameters	Cu-1	Co-1
Empirical formula	$[Cu(C_{10}H_{10}NO_5SBr)(C_{12}H_8N_2)]$. CH_3OH	$[Co(C_{10}H_{10}NO_5SBr)(H_2O)(C_{12}H_8N_2)].CH_3CH_2OH$
Formula weight	611.95	639.38
Temperature (K)	293(2)	293(2)
Wavelength (Å)	0.71073	0.71073
Crystal system,	Monoclinic	Monoclinic
space group	P2(1)/c	I2/a
Unit cell dimensions		
a (Å)	15.516 (8)	15.5234(7)
b (Å)	13.3471 (7)	19.2687(5)
c (Å)	11.7999 (9)	19.1761(8)
β(°)	100.625 (19)	112.933(5)
α, γ(°)	90.00	90.00
V (Å^3)	2401.8 (12)	5282.5(3)
Z, D_{Calcd} (Mg.m^{-3})	4, 1.692	8,1.608
Abs. coefficient (mm^{-1})	2.705	2.29
F(000)	1236	2600
Crystal size (mm^3)	0.30 × 0.15 ×0.08	0.20× 0.08 ×0.05
θ range for data collection	2.3 26.4	3.32, 26.37
Limiting indices	-19 ≤ *h* ≤ 19 -15 ≤ *k* ≤ 16 -14 ≤ *l* ≤ 10	-19 ≤ *h* ≤ 19 -23 ≤ *k* ≤ 24 -23 ≤ *l* ≤ 23
Reflections collected	12394	16529
Independent reflections	4912(R_{int}= 0.0415)	5385(R_{int} = 0.030)
Observed data	3142 (I> 2σ(I))	4202 [I> 2σ(I)]
Refinement method	Refinement on F^2	Refinement on F^2
Nref/Npar/Nres	4912/319/912	5385/343/1018
Final R_1, wR_2, S [I> 2σ(I)]	R_1=0.0647,, wR_2=0.1543, S = 1.032 w = 1/[σ^2(F_o^2)+(0.0785P)^2+3.1072P] where P = (F_o^2 + 2F_c^2)/3	R_1=0.043, wR_2 =0.0998 , S = 1.012 w=1/[σ^2(F_o^2)+(0.0462P)^2+11.5939P] where P = (F_o^2 + 2F_c^2)/3
Final R_1, wR_2, S (all data)	R_1 = 0.1061, wR_2 = 0.1820, S = 1.012	R_1 =0.043, wR_2 =0.110 , S = 0.967

Shiftmax / mean	0.000 / 0.000	0.002 / 0.000

Table S2. Crystal data and structure refinement parameters for Cu-2.

Parameters	Cu-2
Empirical formula	$[Cu_2(C_{10}H_{10}NO_5SBr)_2(H_2O)_2]$. $2H_2O$
Formula weight	871.46
Temperature (K)	296(2)
Wavelength (Å)	0.71073
Crystal system, space group	Monoclinic, P2(1)/c
Unit cell dimensions (Å, °)	
a	12.248(3)
b	7.6422(18)
c	15.829 (4)
α	90.00
β	104.923 (4)
γ	90.00
V (Å^3)	1413.7 (6)
Z, D_{Calcd} (Mg.m^{-3})	2, 2.022
Absorption coefficient (mm^{-1})	4.49
F(000)	868
Crystal size (mm^3)	0.34 × 0.28 ×0.24
θ range for data collection	2.7~ 26.4
Limiting indices	$-14 \le h \le 14$ $-8 \le k \le 9$ $-19 \le l \le 19$
Reflections collected	7738
Independent reflections	2605(R_{int}= 0.043)
Observed data	2267 ($I > 2\sigma(I)$)
Refinement method	Refinement onF^2
Nref/Npar/Nres	8512/727/59
Final R_1, wR_2, S [$I > 2\sigma(I)$]	R_1= 0.0332, wR_2=0.0865 , S = 1.059 $w = 1/[\sigma^2(F_o^2) + (0.0459P)^2 + 1.1448P]$ where $P = (F_o^2 + 2F_c^2)/3$
Final R_1, wR_2, S(all data)	R_1=0.0401, wR_2=0.0896, S = 1.059
Shiftmax / mean	0.001 / 0.000

Table S3. Selected bond distances (Å) and angles (°) for Cu-1、Cu-2 and Co-1.

Cu-1

Bond	Dist. (Å)	Bond	Dist. (Å)	Bond	Dist. (Å)
Cu(1)—O(2)	1.913 (4)	Cu(1)—N(1)	1.937 (5)	Cu(1)—N(3)	1.997 (5)
Cu(1)—N(2)	2.088 (4)	Cu(1)—O(3)	2.202 (5)		
Angle	**(°)**	**Angle**	**(°)**	**Angle**	**(°)**
O(2)-Cu(1)-N(1)	92.78 (18)	O(2)-Cu(1)-N(3)	90.63 (18)	O(2)-Cu(1)-O(3)	105.3 (2)
N(1)-Cu(1)-N(3)	176.34(18)	O(2)-Cu(1)-N(2)	147.98 (18)	N(2)-Cu(1)-O(3)	105.4 (2)
N(3)-Cu(1)-N(2)	80.29 (18)	N(1)-Cu(1)-N(2)	97.45 (18)	N(3)-Cu(1)-O(3)	90.32 (18)
N(1)-Cu(1)-O(3)	87.51 (19)				

Cu-2

Bond	Dist. (Å)	Bond	Dist. (Å)	Bond	Dist. (Å)
Cu(1)—O(2)	1.892 (2)	Cu(1)—O(1W)	1.9793 (10)	Cu(1)—O(3)	1.975 (2)
Cu(1)—N(1)	1.9479	Cu(1)—O(5) ^{i}	2.333 (3)		
Angle	**(°)**	**Angle**	**(°)**	**Angle**	**(°)**
O(2)-Cu(1)-N(1)	94.02 (8)	O(1W)-Cu(1)-O(5)i	88.08 (8)	O(2)-Cu(1)-O(3)	155.42 (12)
O(2)-Cu(1)-O(1W)	86.82 (8)	O(3)-Cu(1)-O(1W)	85.40(8)	N(1)-Cu(1)-O(1W)	177.23 (7)
O(2)-Cu(1)-O(5)i	100.82(11)	O(3)-Cu(1)-O(5)i	102.17 (12)	N(1)-Cu(1)-O(5) i	89.17 (8)
N(1)-Cu(1)-O(3)	94.86 (9)				

Co-1

Bond	Dist. (Å)	Bond	Dist. (Å)	Bond	Dist. (Å)
Co(1)—O(2)	1.991 (2)	Co(1)—N(1)	2.091 (2)	Co(1)—O(3)	2.103 (2)
Co(1)—O(1W)	2.116 (2)	Co(1)—N(3)	2.147 (3)	Co(1)—N(2)	2.178(2)
Angle	**(°)**	**Angle**	**(°)**	**Angle**	**(°)**
O(2)-Co(1)-N(1)	89.69 (9)	O(2)-Co(1)-O(3)	177.26 (8)	N(1)-Co(1)-O(3)	91.44 (9)
O(2)-Co(1)-O(1W)	91.63 (8)	N(1)-Co(1)-O(1W)	96.51 (9)	O(3)-Co(1)-N(3)	85.89 (9)
O(2)-Co(1)-N(3)	93.33 (9)	N(1)-Co(1)-N(3)	171.48 (10)	N(3)-Co(1)-N(2)	77.32(10)

O(1 W)-Co(1)-N(3)	91.37 (10)	O(2)-Co(1)-N(2)	94.85(9)	O(3)-Co(1)-O(1W)	85.77 (8)
O(3)-Co(1)-N(2)	87.55(9)	O(1W)-Co(1)-N(2)	167.25(9)	N(1)-Co(1)-N(2)	94.50(10)

Symmetry code: (i) −x, −y, −z+1.

Table S4. Hydrogen bond lengths (Å) and angles (°)for Cu-1 and Co-1.

Cu-2

D—H••• *A*	*D*—H	H ••• *A*	*D* ••• *A*	<*D*H*A*
O(1W)—H(1WB) ••• O(5) i	0.85	2.67	3.009(3)	105
O(1 W)—H(1WA) ••• O(4) ii	0.85	2.16	2.756(3)	127
O(2W)—H(2WA) ••• O(1W) iii	0.85	1.92	2.714(3)	156
O(2W)—H(2WB) •••Br1 iv	0.85	2.96	3.671	143

Co-1

D—H••• *A*	*D*—H	H ••• *A*	*D* ••• *A*	<*D*H*A*
O(1W)—H(1WA) ••• $O2^{i}$	0.848 (9)	1.907 (11)	2.741 (3)	168 (3)
O(1W)—H(1WB) ••• $O6^{ii}$	0.846 (9)	1.950 (12)	2.783 (3)	168 (3)
O6—H6••• $O5^{iii}$	0.82	2.00	2.813 (4)	172
O6—H6••• $S1^{iii}$	0.82	2.84	3.533 (3)	144

Symmetry codes:

For complex Cu-2: (i) −*x*, −*y*+1, −*z*+1; (ii) *x*, −*y*+1/2, *z*+1/2; (iii) −*x*+1, *y*+1/2, −*z*+3/2;

(iv) −*x*, −*y*, −*z*+1.

For complex Co-1: (i) −*x*+3/2, *y*, −*z*+2; (ii) *x*, −*y*+1/2, *z*+1/2; (iii) *x*, −*y*+1/2, *z*−1/2.

Supporting Figures

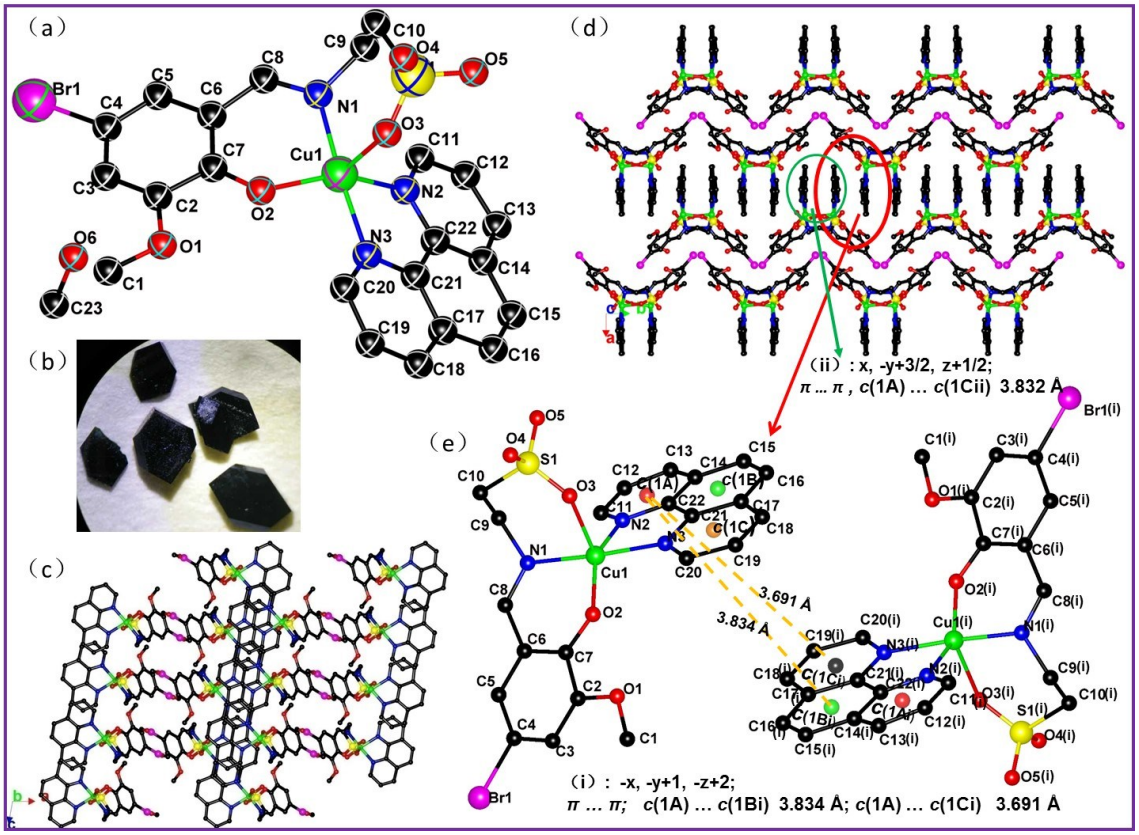

Figure S1. (a) Molecular view of Cu-1 using atoms labelling scheme, and ellipsoids were drawn at the 50% probability level; (b) The single crystal morphology of Cu-1; (c) A view of 2-D sheet structure of Cu-1 in *ac* plane; (d) A view of 2-D layer structure of Cu-1 in *ab* plane; (e) A view of π... π stacking in the of structure of Cu-1 [Symmetry codes: (i) −x, −y+1, −z+2].Some H atoms were omittedfor clarity.

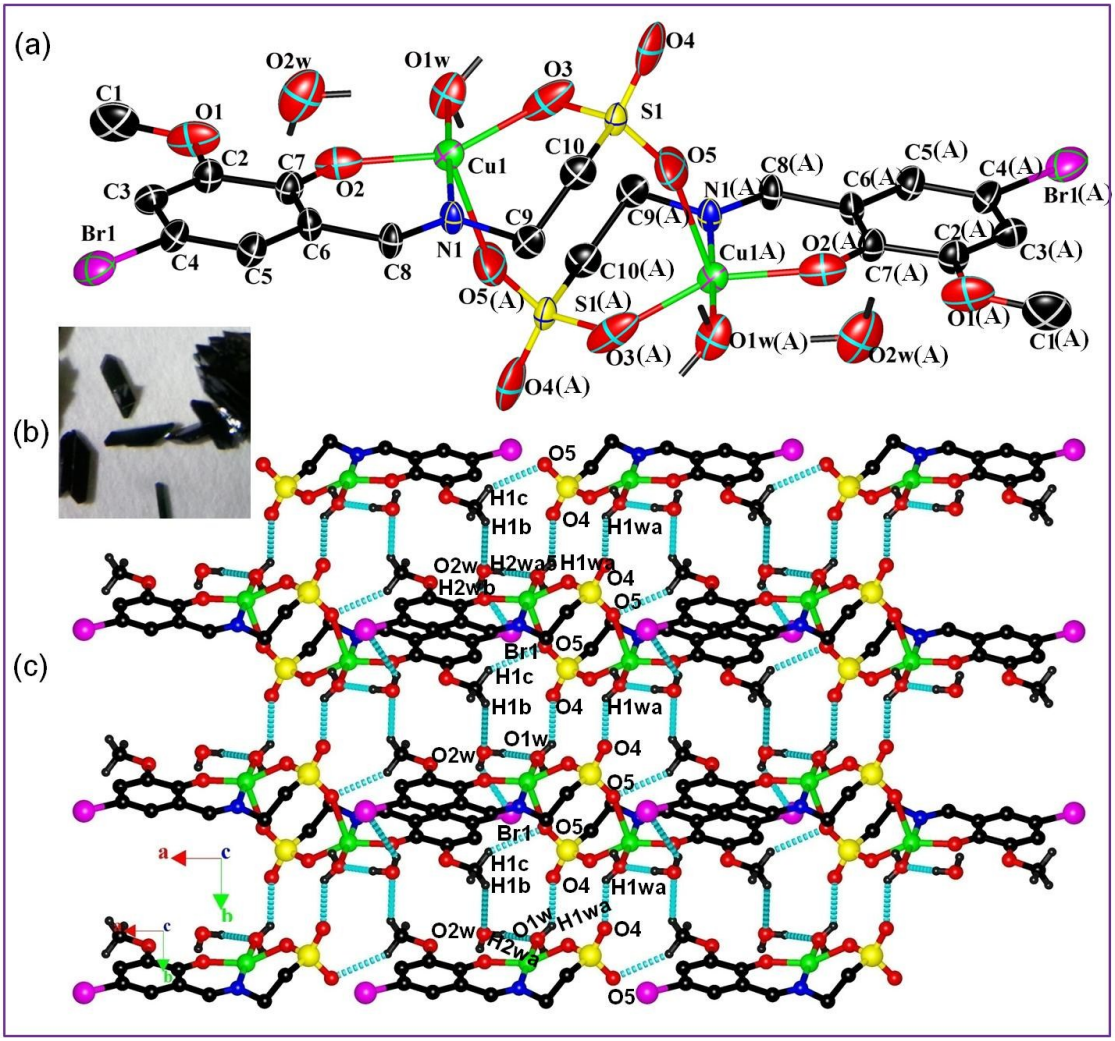

Figure S2. (a) Molecular view of Cu-2 using atoms labelling scheme, and ellipsoids were drawn at the 50% probability level (Symmetry codes: (i) −x, −y, −z+1); (b) The single crystal morphology of Cu - 2; (c) A view of 2-D stratified structure of Cu-2 in *ab* plane. Some H atoms were omittedfor clarity. Dashed lines are hydrogen bonds in (c).

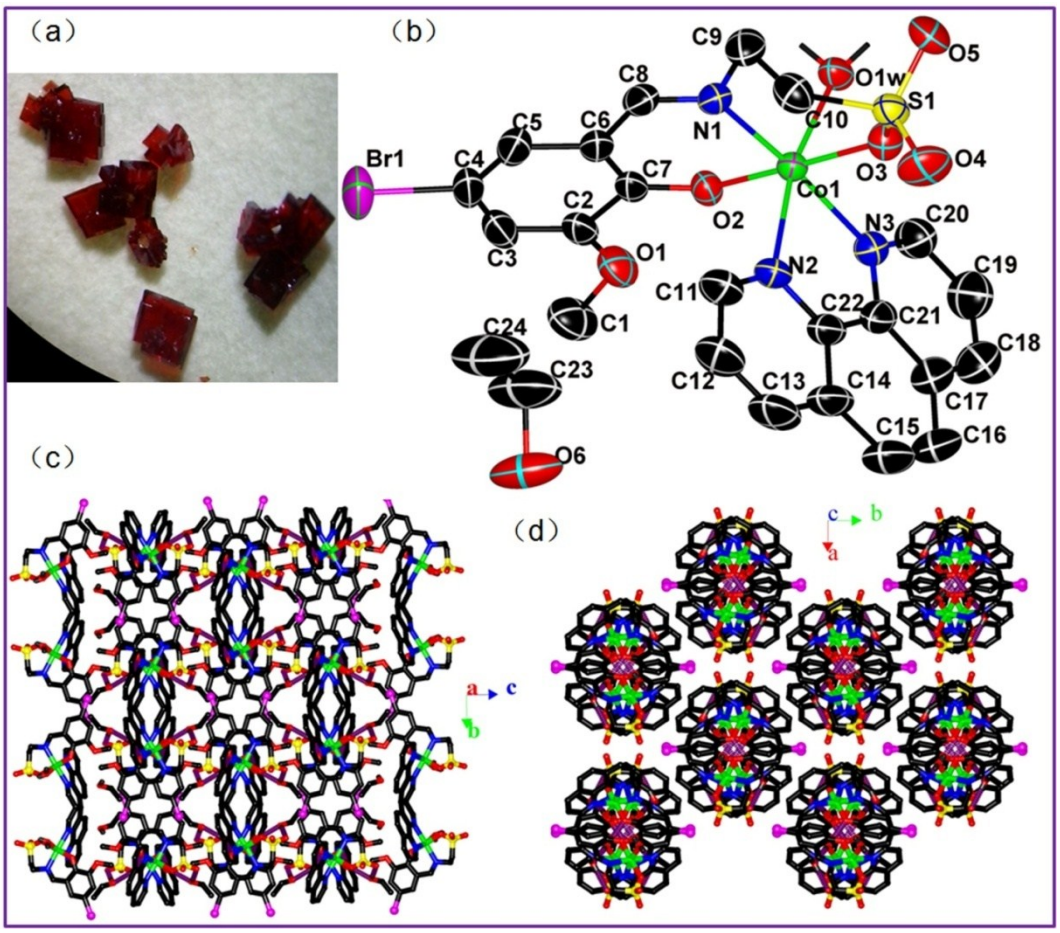

Figure S3. (a) The single crystal morphology of Co-1; (b) Molecular view of Co-1 using atoms labelling scheme, and ellipsoids were drawn at the 50% probability level; (c) A view of 2-D net structure of Co-1 in *bc* plane; (c) A view of 2-D sheet structure of Co-1 in *ab* plane. Some H atoms were omitted for clarity.

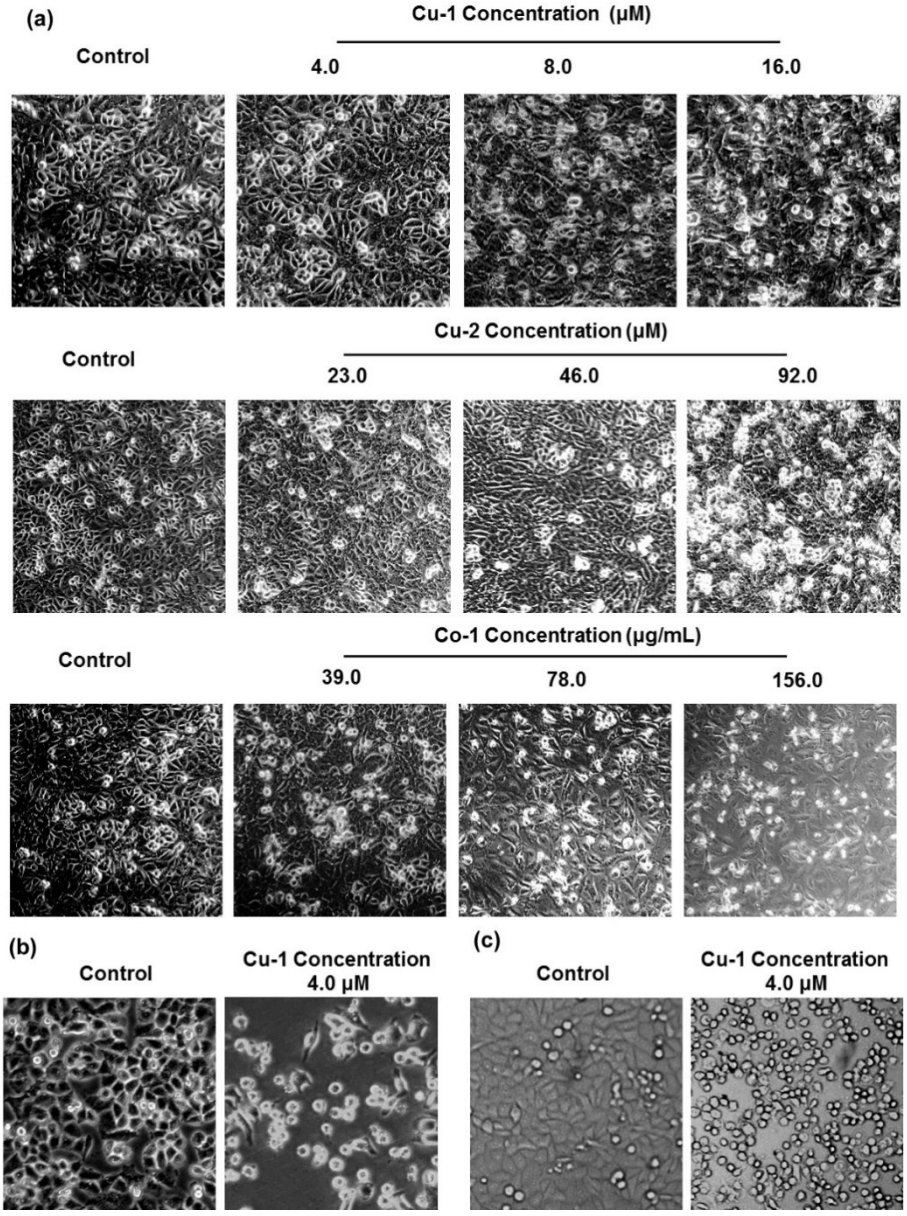

Figure S4. (a)The change in morphology of HUVECs in presence of Cu-1, Cu-2, and Co-1 with the varied concentration for 48 h; (b) The change in morphology of C33A cells in presence of Cu-1 with concentration 4.0μM for 48 h; (c) The change in morphology of HeLa cells in presence of Cu-1 with concentration 4.0μM for 48 h. The images were taken with an inverted microscope(HUVECs: 10× magnification; C33Acells: 20×magnificatio, and HeLa cells: 10×magnification).

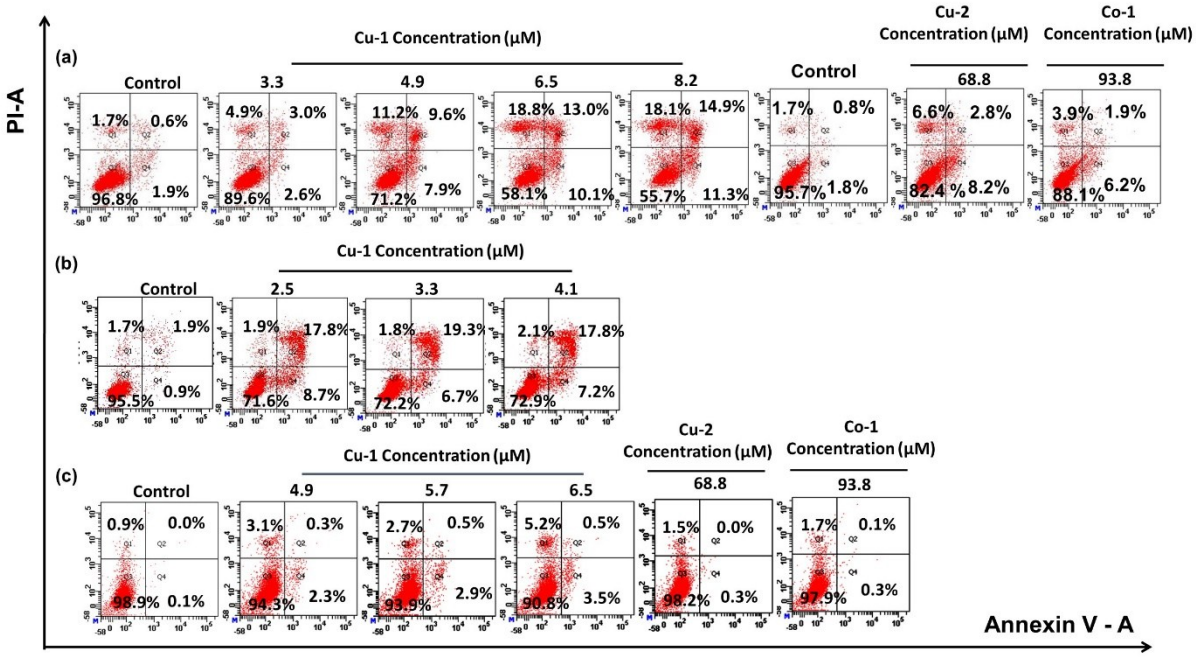

Figure S5. C33A cells, HeLa cells and HUVECs were double stained with annexin V/PI, respectively. (a) Induced apoptosis of C33A cells (a), HeLa cells(b) and HUVECs (c) were analysed by flow cytometry after the cells were treated with different concentrations of Cu-1，Cu-2 and Co-1for 20 h. This figure shows one of the three independent experiments.

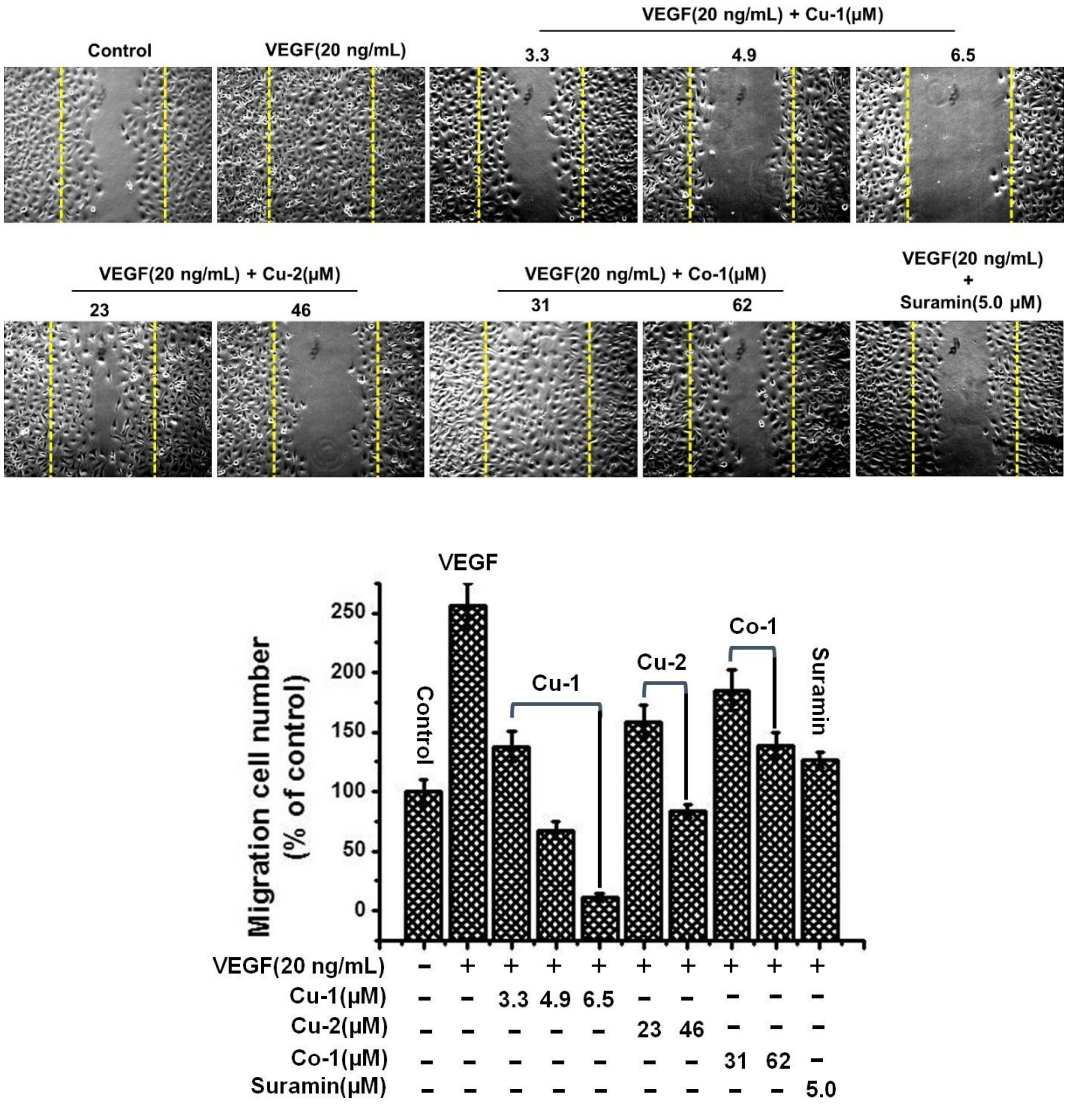

Figure S6. Effects of Cu-1, Cu-2, Co-1, and suramin on HUVECs migration in wound migration assays in the presence of VEGF stimulation. Cells were wounded with a pipette tip. After cells were incubated for 24 h, images of HUVEC wound migration were taken with an inverted photomicroscope at 10 × magnification. After incubation, the number of migration cells was quantified by manual counting. These experiments were performed thrice with similar results, and significant differences from control group were observed. Data were presented as the percentages of the control group, which was set at 100%.Cu-1is more advantageous than Cu-2, Co-1, and suramin in inhibiting the migrations of inactivated HUVECs in a dose-dependent manner in the presence of VEGF stimulation. Suramin is a positive control.

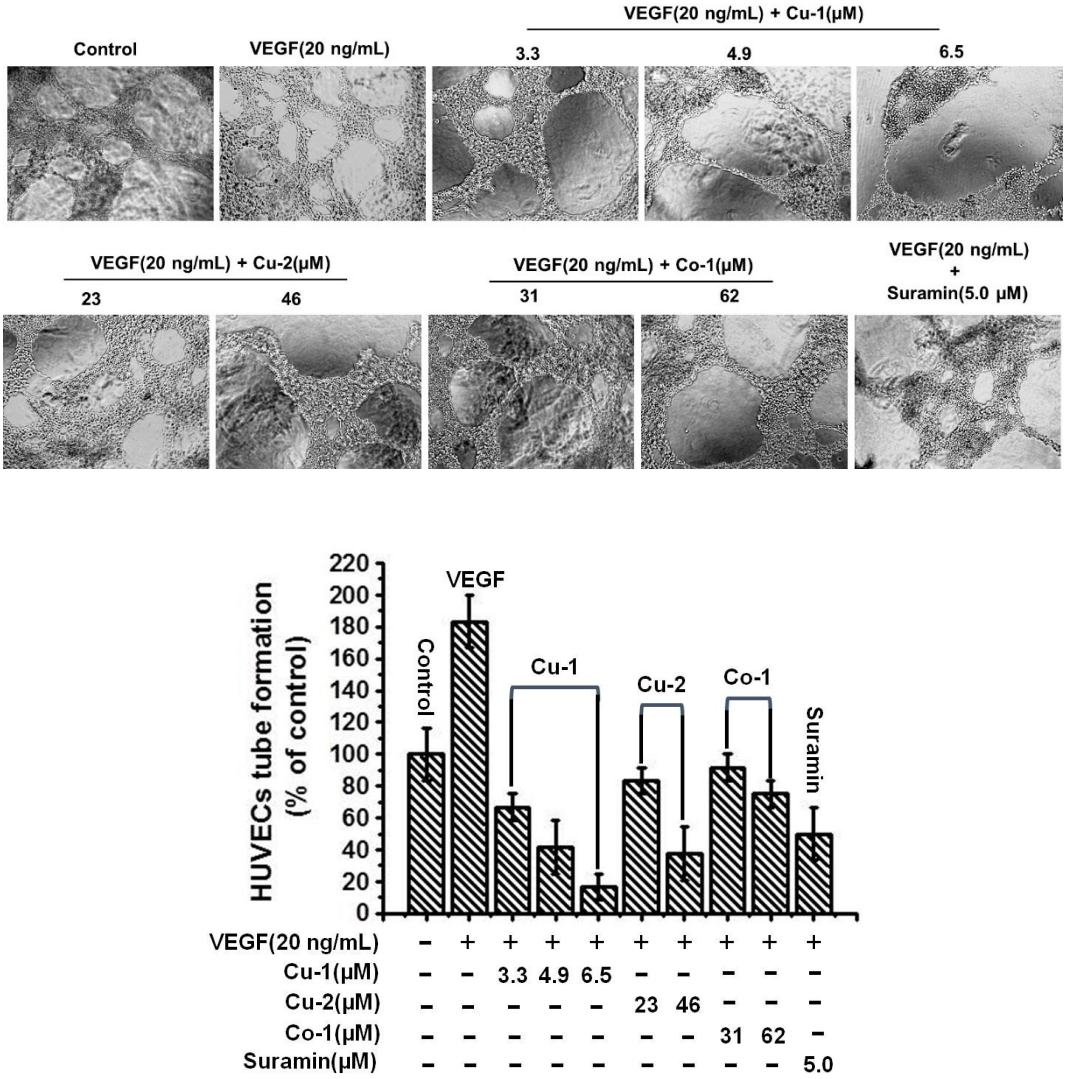

Figure S7. Effects of Cu-1, Cu-2, Co-1, and suramin on HUVECs tube formations in the presence of VEGF. HUVECs (4.0×10^4) were treated by Cu-1, Cu-2, Co-1, and suramin in the presence of VEGF, and were added on matrigel layers. After cells were incubated for 12 h, images of HUVEC tube-like formations were taken with an inverted photomicroscope at 10 × amplification. The tube-like formations were quantified by manual counting. These experiments were performed thrice with similar results, and significant differences from control group were observed ($p < 0.05$). Data are presented as the percentages of the control group, which was set at 100%. Cu-1is more advantageous than Cu-2, Co-1, and suramin in inhibiting tube formations of HUVECs in a dose-dependent manner in the presence stimulation of VEGF. Suramin is a positive comparison.

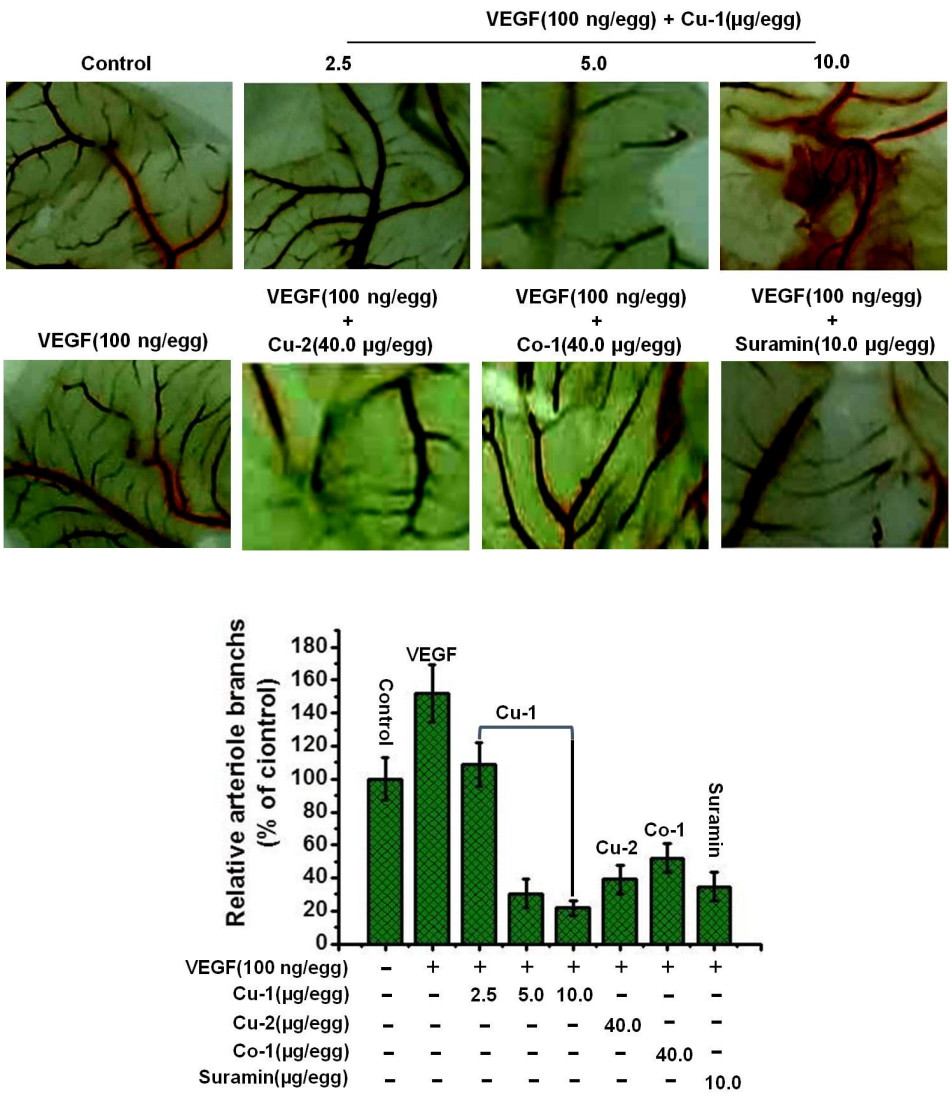

Figure S8. Angiogenic development of the arterial endpoint in the chick embryowas stimulated by VFGF and was inhibited by Cu-1,Cu-2, Co-1, and suramin. The chick embryos were treated with PBS (Control), VFGF; VFGF + Cu-1, VFGF + Cu-2, VFGF + Co-1, and VFGF + suramin, respectively. The various test compounds were injected into the chick embryo of fertilized chicken eggs on day 7 of development, and the anti-angiogenic effects of the test compounds were observed at 4d after injection. The images were taken with a mobile phone (OPPO R9t).The arteriole branchs were quantified by manual counting. These experiments were performed thrice with similar results and significant differences from control group were observed($p < 0.05$). Data were presented as the percentages of the control group, which was set at 100% . Suramin is a positive comparison.

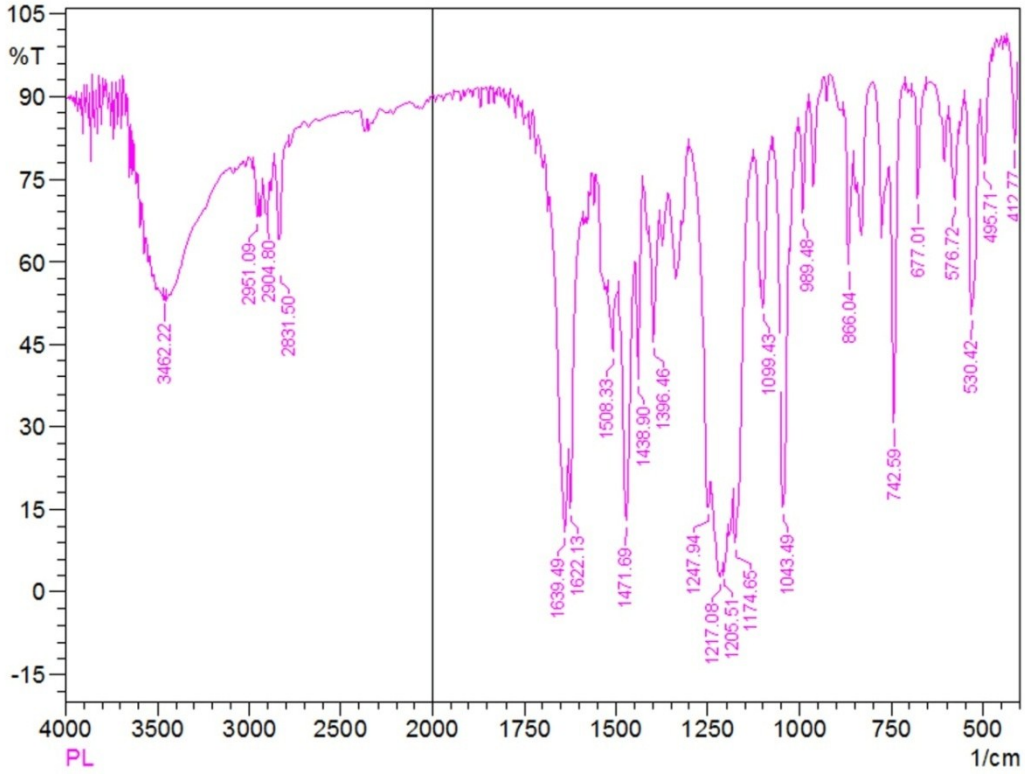

Figure S9. FT-IR of Schiff base ligand.

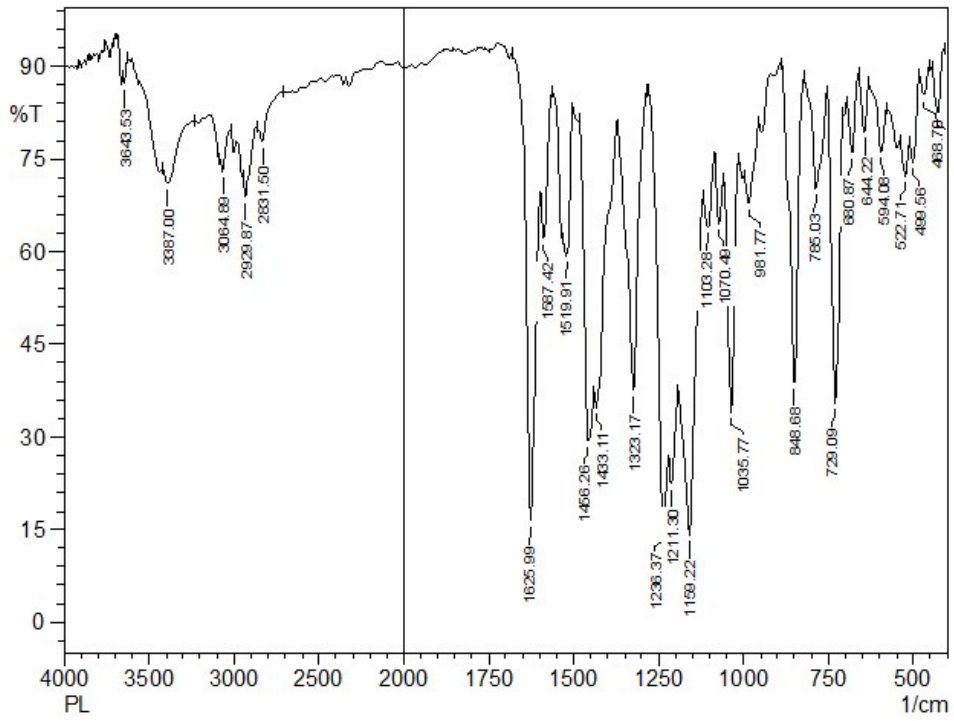

Figure S10. FT-IR of Cu-1.

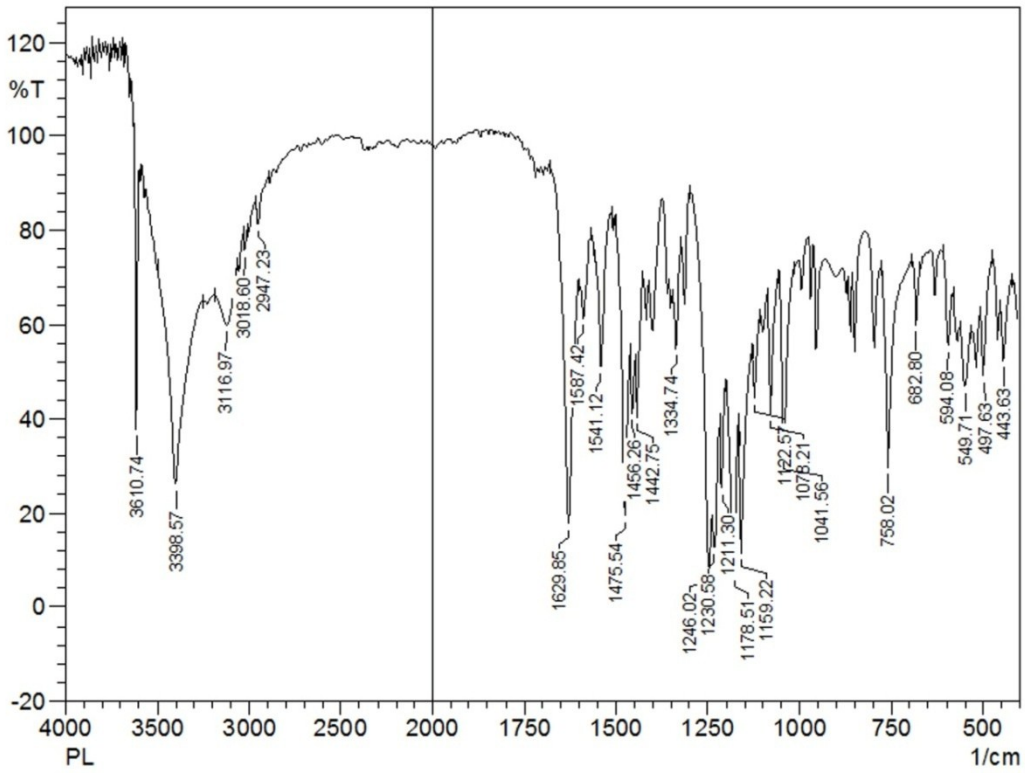

Figure S11. FT-IR of Cu-2.

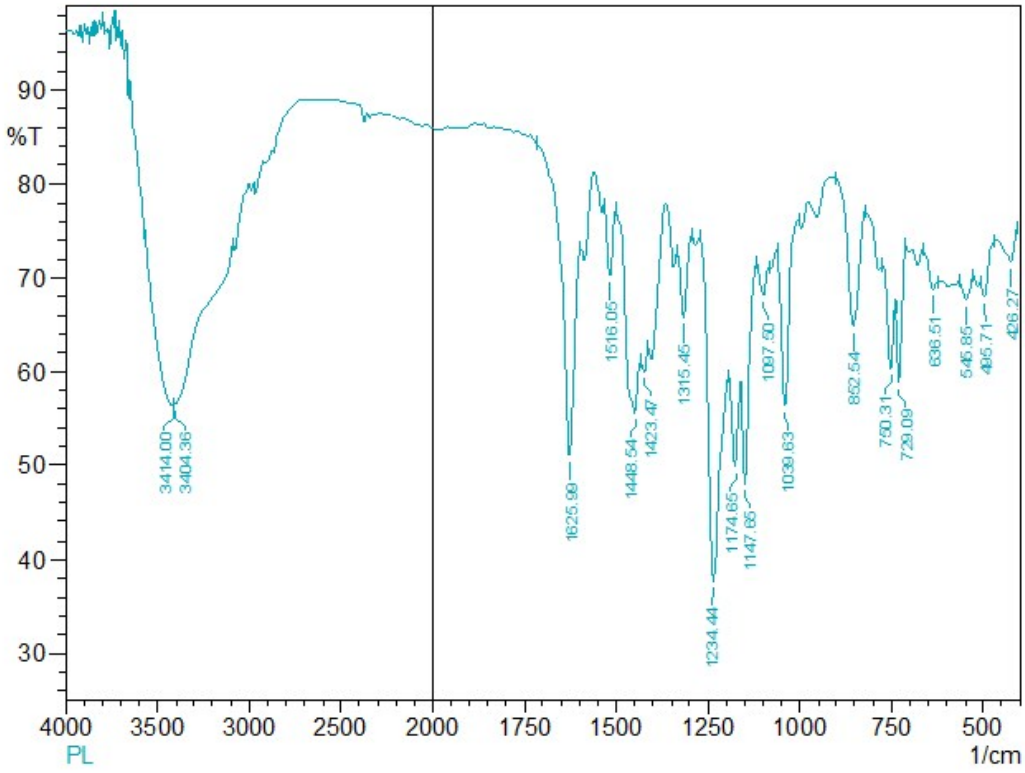

Figure S12. FT-IR of Co-1.

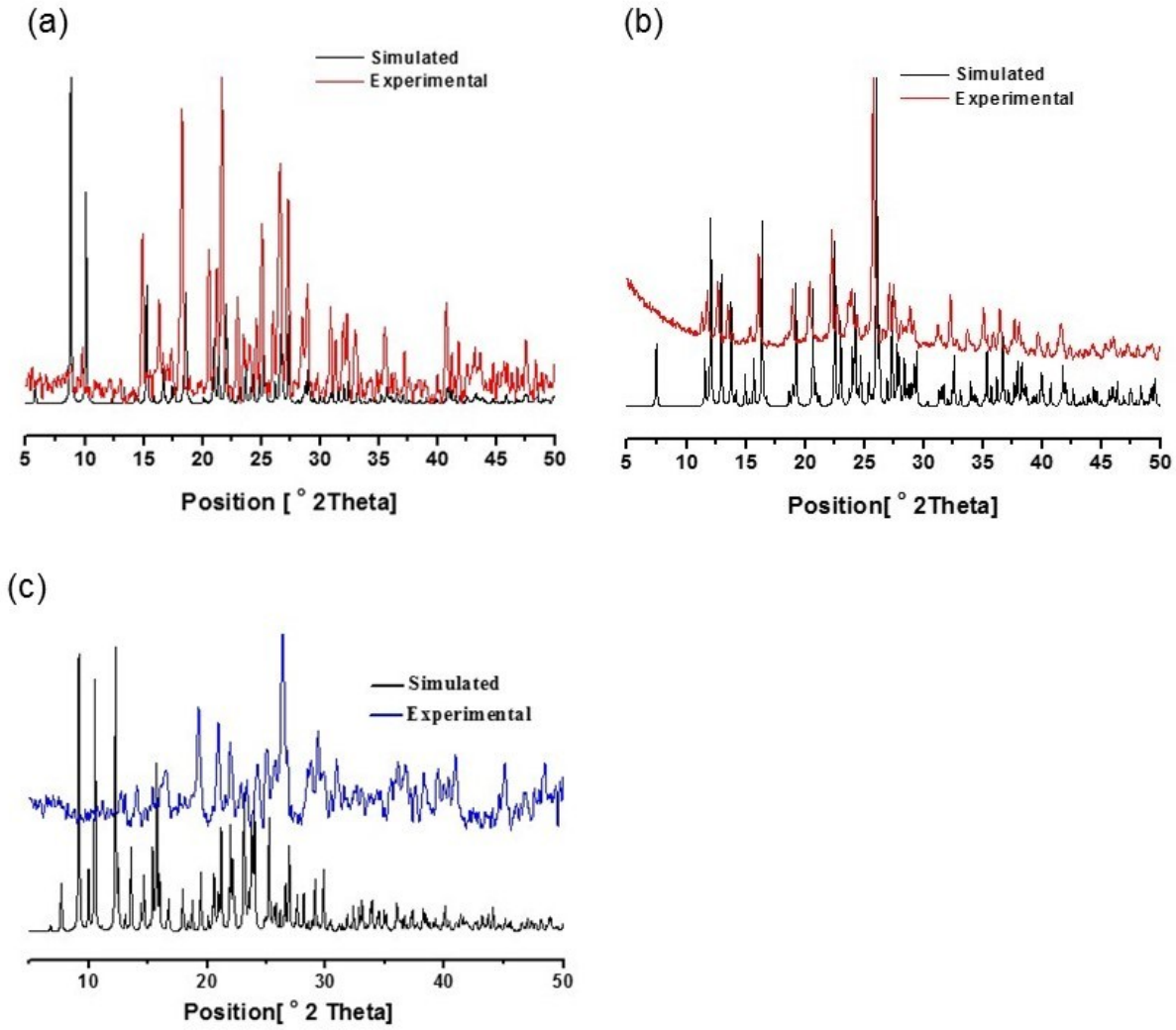

Figure S13. The powder diffractograms and theirsimulated diffractogramsgenerated from single crystal X-ray diffraction data.(a) Cu-1; (b) Cu-2; (c) Co-1.

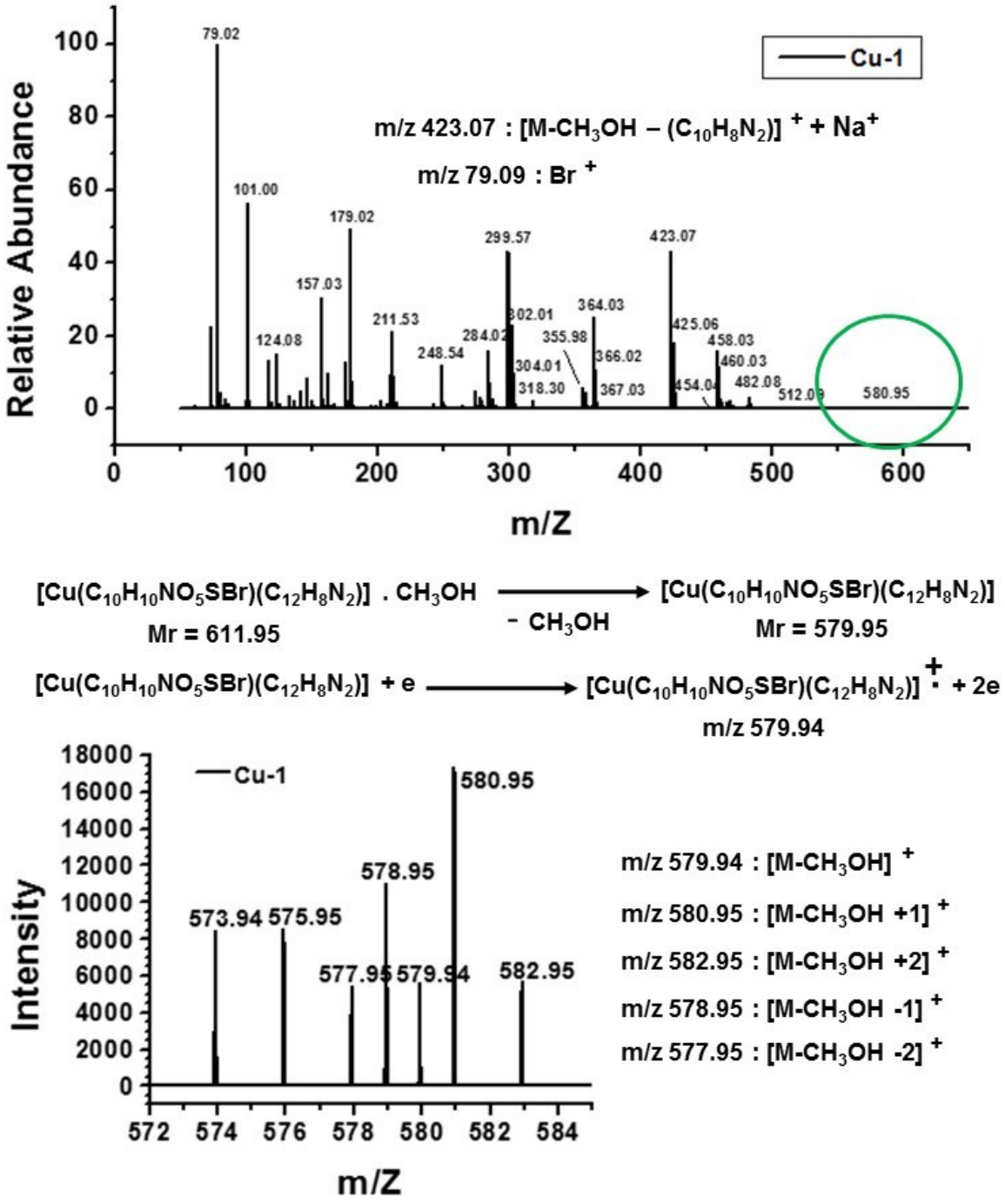

Figure S14. Liquid Chromatography Mass Spectrometry of positive ion of Cu-1.

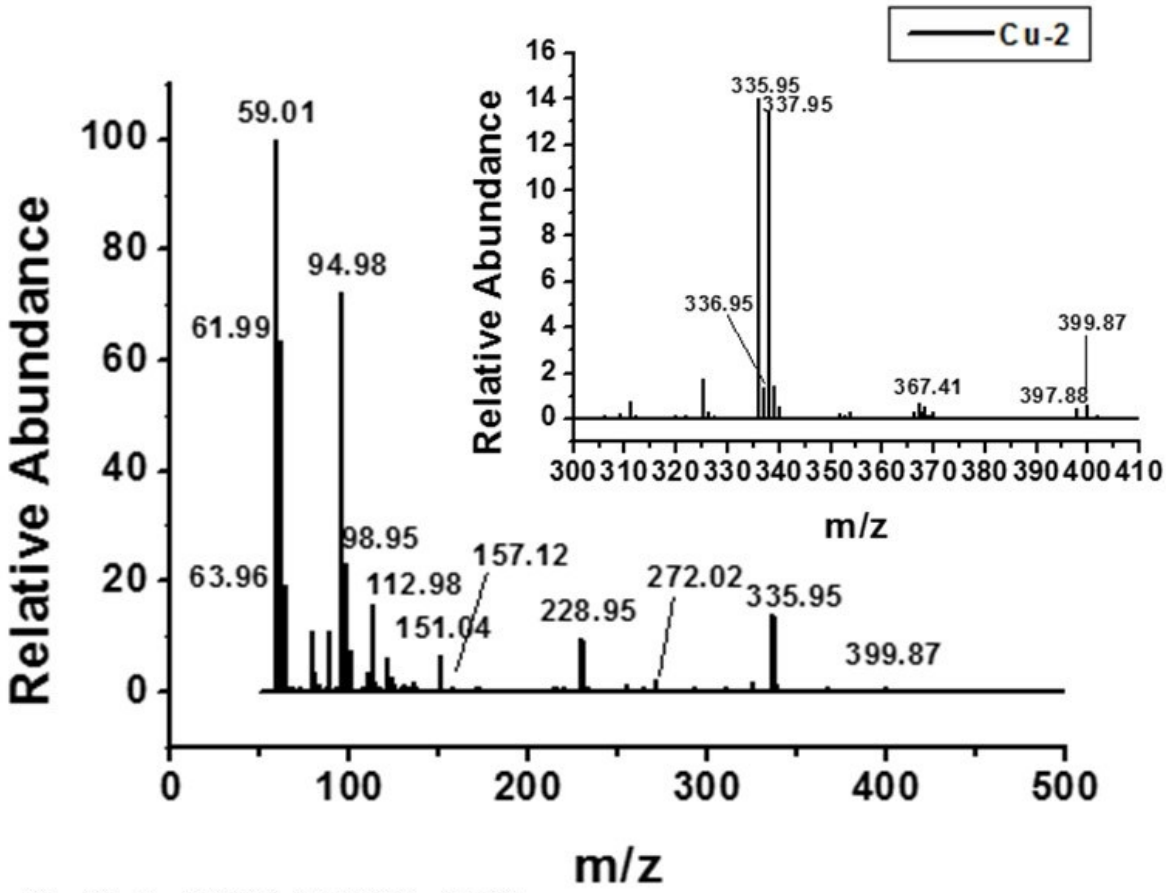

$[Cu_2(C_{10}H_{10}NO_5SBr)_2(H_2O)_2]\ .\ 2H_2O$

Mr = 871.46

m/z 335.95 $[(C_{10}H_{10}NO_5SBr)\ -1]^{2-}$: 1/2 $[M-4H_2O-\ 2Cu]^{2-}$

m/z 337.95 $[(C_{10}H_{10}NO_5SBr)\ +1]^{2-}$: 1/2 $[M-4H_2O-\ 2Cu]^{2-}$

m/z 399.87 $[Cu(C_{10}H_{10}NO_5SBr)]^{2-}$: 1/2 $[M-4H_2O]^{2-}$

m/z 397.88 $[Cu(C_{10}H_{10}NO_5SBr)-2]^{2-}$: 1/2 $[M-4H_2O-2]^{2-}$

Figure S15. Liquid Chromatography Mass Spectrometry of positive ion of Cu-1.

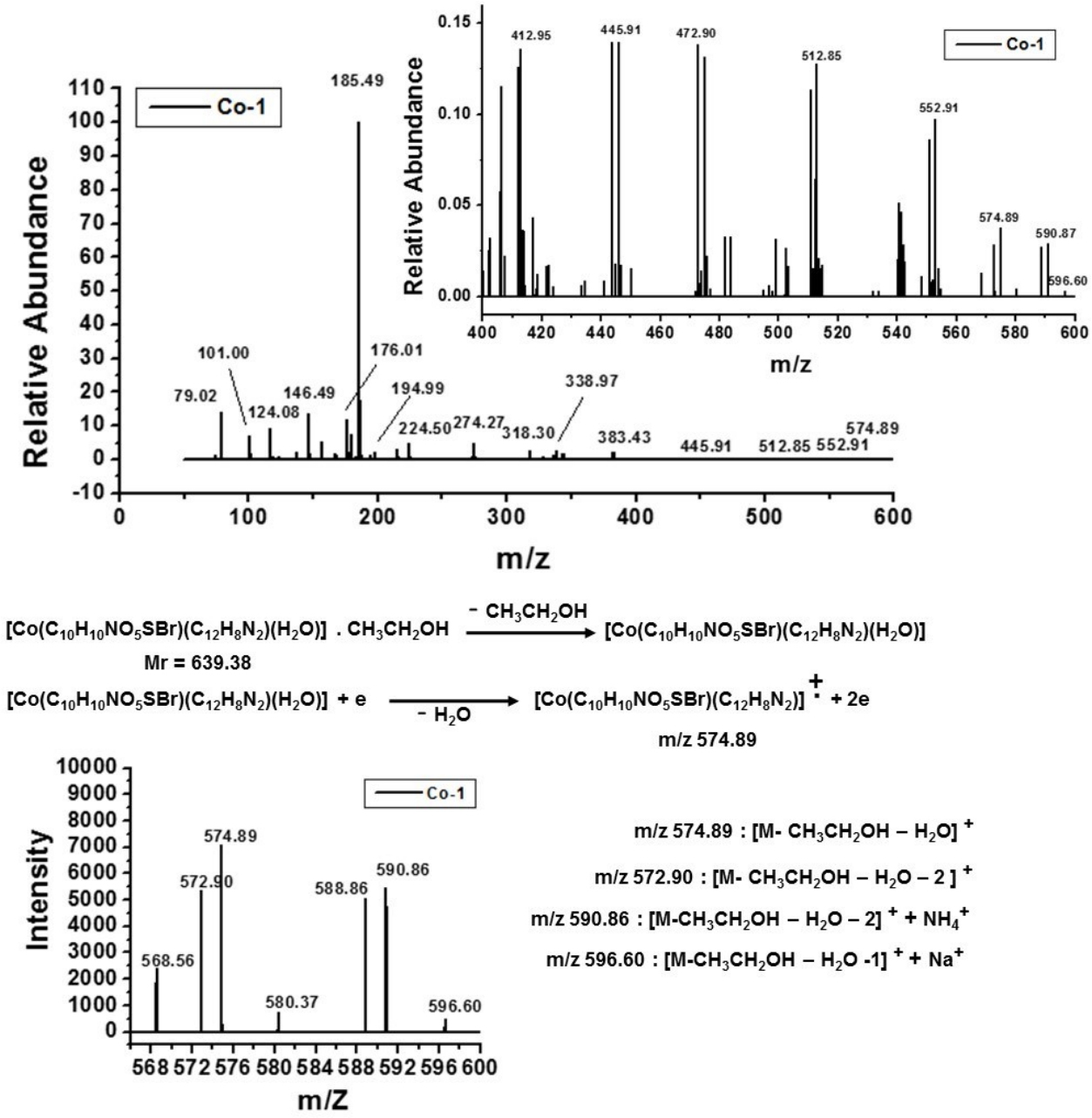

Figure S16. Liquid Chromatography Mass Spectrometry of positive ion of Co-1.